Int J Adv Manuf Technol (2018) 94:3853–3861
DOI 10.1007/s00170-017-1076-5

ORIGINAL ARTICLE

Adaptive real-time model on thermal error of ball screw feed drive systems of CNC machine tools

Tie-jun Li[1,2] · **Chun-yu Zhao**[1] · **Yi-min Zhang**[1,2]

Received: 21 February 2017 / Accepted: 12 September 2017 / Published online: 26 September 2017

Abstract The positioning error of ball screw feed drive systems is mostly caused by thermal deformation of the ball screw shaft in machine tool feed systems. This paper presents an adaptive real-time model (ARTM) for predicting the temperature transient distribution and thermal error distribution of the ball screw shaft. FEM integrated with the Monte Carlo method is applied to determining the heat generation rates of two bearings, moving nut and two guides in the ball screw feed system. Then based on the data of the FEM calculations, an exponential function of the feed velocity and time is used to describe variation of the temperature difference between the measured surface point and the center of the kinematical pair with time. Finally, a numerical forecasting algorithm is developed to predict the thermal characteristics of the screw shaft and its effectiveness is verified by the experiments.

Keywords Ball screw · Machine tool · Heat generation rate · Finite element method · Monte Carlo method · Thermal error

1 Introduction

Machine tools and their components are sensitive to temperature change that could exert an influence on mechanical structure deformation thereby inducing thermal error of motion drive systems and reducing the geometrical and machining accuracy [1]. According to statistics, thermally induced error can account for about 40–70% the total errors arising from various error sources [2, 3]. Therefore, the topics of thermal error in machine tools have been the focus of significant recent research activities, including measurement of temperatures and displacements, computations of thermal errors of machine tools and reduction of thermal errors [4–17].

Of all factors that contribute to the thermal error of a machine tool, thermal error of ball screw system plays a very important role [1]. In order to investigate thermal behavior of the ball screw system, experimental measurement of temperature variation and positioning error along the screw, theoretical modeling of the physical process and the heat sources causing the thermal deformation of the ball screw are frequently preformed. Temperature measurement is important to get a better understanding of thermal errors of the ball screw system. The temperatures are measured using thermocouples while a laser interferometer and a capacitance probe are applied to measure the thermal error of the ball screw [18]. Usually, three thermocouples respectively located on surroundings, and the rear and front bearings are used for continuously recording the room temperatures and the surface temperatures of two support bearings under moving conditions [18, 19]. The other temperature distribution along the ball screw can be measured with infrared radiation thermocouples or an infrared thermographic camera [19, 20].

The source of thermal error in the ball screw transmission is the thermal changes in the active length of the screw. In order to investigate the thermal effect, theoretical modeling and analysis based on numerical simulation are frequently performed. In the course of these researches, the finite element method (FEM) [17–19, 21–23] and the finite difference method (FDM) [4] have often been employed to estimate the thermal behavior of machine tool. Kim et al. evaluated the eventual thermal error of a ball screw system using separately

✉ Chun-yu Zhao
chyzhao@mail.neu.edu.cn

[1] School of Mechanical & Automation, Northeastern University, Shenyang 110819, China

[2] Department of Mechanical Engineering, Shenyang University of Chemical Technology, Shenyang 110142, China

modeling thermal behaviors of the ball screw and the guide way, in which the ball screw was modeled by applying the modified lumped capacitance method (MLCM), while the thermal deformation of the guide way was evaluated using FEM with boundary conditions obtained experimentally [19, 24]. However, accurate modeling of the heat source is quite difficult because the thermal changes depend on the type and dimension of the screw, the tension of the turning parts, the nut and the bearings, the external load, the rotational speed, the work cycle, the load resulting from the torque of elastohydrodynamic friction in the lubricating film of the turning parts, and the heat transfer conditions [4].

This paper aims to develop an adaptive real-time model for predicting the thermal characteristics of the ball screw drive system on line. In the next section, a FEM integrated with the Monte Carlo method is described. The ARTM and the experimental setup are presented in Sections 3 and 4, respectively. The numerical results are discussed in Section 5, and conclusions are provided in Section 6.

2 Finite element model integrated with the Monte Carlo method

2.1 Heat generation and the finite element model

The main heat source of a ball screw feed system is the friction caused by the kinematical pairs, such as nut and shaft of the ball screw, rotating bearings, and rail and slider of guides. In particular, the heat generation caused by the friction is dependent upon feed velocity, lubricant, and assembly conditions [4, 19], which results in the coherence changes of temperature distribution and thermal deformation along the ball screw. However, it is difficult to measure the temperatures directly owing to the ball screw and the centers of kinematical pairs. Therefore, numerical simulation is frequently required to determine the temperature distribution or deformation along the ball screw. In this paper, as the combined analysis of deformation and temperature distribution of the ball screw system, temperature distribution is calculated using the FEM based on the following assumptions [19, 21, 22]:

1. The friction heat generated between the moving nut and the screw is uniform, and a fixed ratio of the heat generated between the screw shaft and the nut is supposed to be transferred to the ball screw shaft.
2. The screw shaft is simplified to be a solid cylinder with a uniform heat generation rate.
3. The support bearings are hollow cylinders.
4. The friction heat between the guide and the sliders is uniform. A fixed ratio of the heat generated between the guide and the sliders is supposed to be transferred to the guide.
5. The radiation term can be neglected for smaller temperature increases.
6. Convective heat coefficients are always constant during motion at the same feed rate.

Figure 1 shows the z-axis worktable of the object CNC lathe modeled with ANSYS software, on which the x-axis worktable moves forward and backward. The system consisted of the following components: a servomotor, supporting bearings 1 and 2, a screw shaft and a nut, and guiders 1 and 2. SOLID87 solid elements were chosen to calculate the temperature field of the ball screw system and the worktable, while CONTA174 contacting elements were used to simulate the contact areas. There are totally 42,512 solid elements and 23,448 contact elements.

As illustrated in Fig. 1, there were three fixed heat sources, the servomotor, and bearings 1 and 2. Here heat generation of the servomotor was amalgamated into bearing 1 and their heat generation rate was denoted by Q_{B1}. The heat generation rate of the bearing 2 was denoted by Q_{B2}. There were also three moving heat sources of the nut, guides 1 and 2, the heat generation rates of which were considered to be only that the parts of their friction heat were transferred to the considered model and denoted by Q_n, Q_{g1} and Q_{g2}, respectively. Due to the symmetry of the model in Fig. 1, it was assumed that $Q_{g1} = Q_{g2} = Q_g$.

2.2 Heat transfer from the feed drive system into the ambient air

1. Heat transfer coefficient for convection of the screw shaft.

Heat dissipates from the ball screw shaft into the ambient air through forced convective heat transfer. The calculation of the heat transfer coefficient for convection follows a series of steps. First, the mean velocity of the fluid with respect to the solid surface is determined. When the parameter is known, the Reynolds number is determined. For the ball screw shaft rotating at an angular velocity of ω, the Reynolds number is written as

$$R_e = \frac{\omega d^2}{2\nu_{fluid}} \tag{1}$$

where ν_{fluid} is the kinematic viscosity of the air, and d is the diameter of the screw shaft.

Second, the Nusselt number is determined by

$$N_u = 0.133 R_e^{2/3} P_r^{1/3} \tag{2}$$

where the Prandtl number P_r is a material parameter of the fluid and calculated as [7].

$$P_r = \frac{C_{fluid}\mu_{fluid}}{\lambda_{fluid}} \tag{3}$$

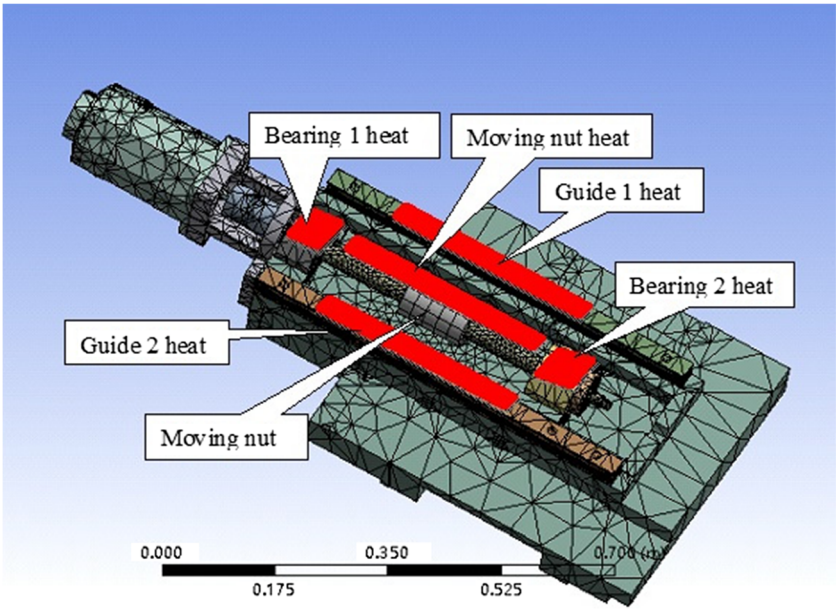

Fig. 1 Finite element model and heat source distribution of the ball screw system

where C_{fluid} is the specific heat capacitance of the air, μ_{fluid} is the dynamic viscosity of the air, and λ_{fluid} is the thermal conductivity of the ambient air. For the air, $P_r = 0.707$ [20].

Then, the heat transfer coefficient is expressed as

$$h = \frac{N_u \lambda_{\text{fluid}}}{d}. \tag{4}$$

2. Heat transfer coefficient for convection of the bed saddle.

The effect of air flow velocity on the convective heat transfer coefficient can be neglected because the feed speed of the bed saddle is relatively low. A convective heat transfer coefficient of 12 W/m^2 K is used for the surfaces of the bed saddle and the bearing seats and housing [4].

2.3 Implementation of the FEM integrated with the MC method

The Monte Carlo (MC) method is also called stochastic simulation method [25]. Herein, the MC method is used for simulating the real heat generation rates, Q_{B1}, Q_{B2}, Q_n, and Q_g, which are denoted by x_1, x_2, x_3, and x_4, respectively. In order to determine these four parameters, an experiment was conducted to measure the temperature variations of 15 given points on the surfaces of the object worktable with time. The given points are denoted by T1, T2, ⋯, T15 in Fig. 2 and the experimental procedure will be described in Section 4. The idea to determine the heat generation rates is to "match" the measured temperatures of the given points to the results of the FEM calculation. The way to match the two results is through the least squares of the differences between them. In other word, the computational procedure is to find the four parameters that minimize the following functional expression:

$$F(x_1, x_2, x_3, x_4) = \sum_i \sum_j \left(T_{ij}^{\text{EM}} - T_{ij}^{\text{MC}} \right)^2 \tag{5}$$

where T_{ij} is the temperature for given point i at the jth sampling time step of t_j, $i = 1, 2, \cdots, 15$, and $j = 1, 2, \cdots, N$; the superscripts EM and MC denote the values of experimental measurement and the FEM/ MC simulation, respectively.

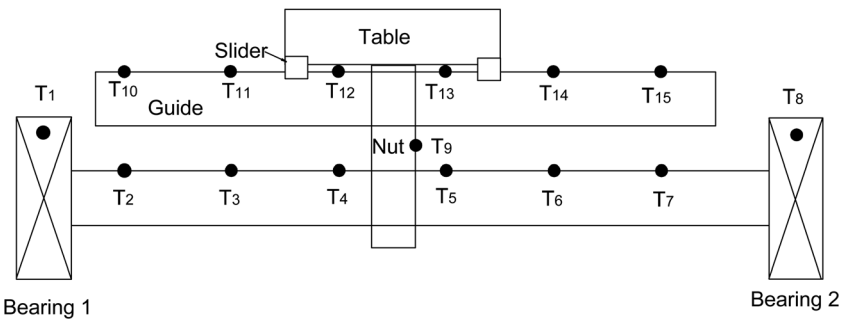

Fig. 2 Locations of temperature measurement points for the ball screw system

The computational procedure is represented as a flow chart in Fig. 3. The Monte Carlo simulation can be regarded as a sampling process and will be repeated for a given sampling times k. The amount of k should be big enough in order to enhance the calculation accuracy. Here, the function *random* (m, n) in ANSYS APDL is used to generate a random number between m and n. If the parameter x_l is distributed in the interval of $[x_{Ll}, x_{Ul}]$, the heat generation rates of one sampling time are expressed as

$$x_l = x_{Ll} + random(0, \delta_l), \delta_l = x_{Ul} - x_{Ll}, l = 1, 2, 3, 4. \quad (6)$$

After each sampling time of the four heat generation rates, the calculation of the FEM is performed to extract

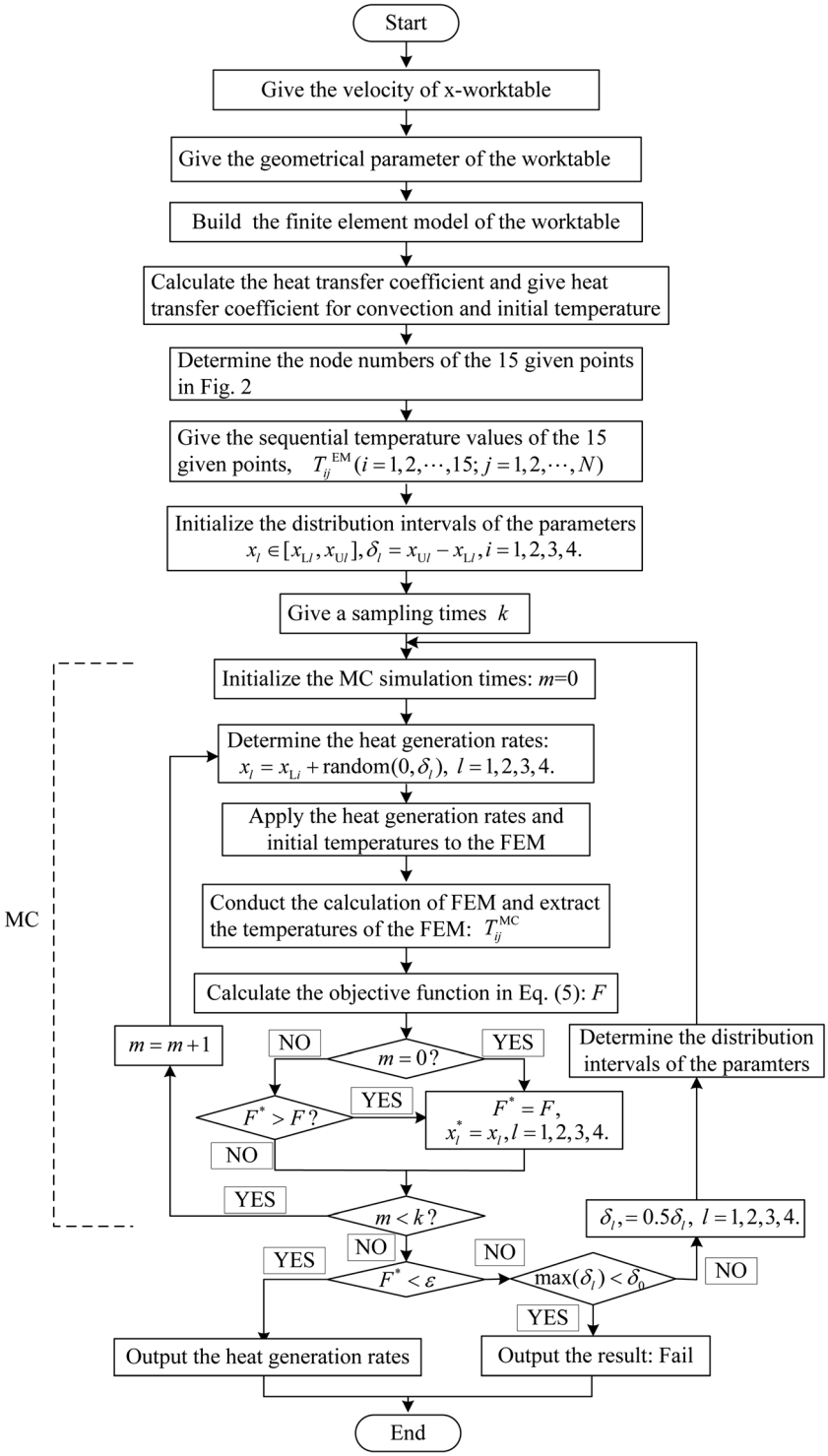

Fig. 3 Flowchart of the FEM/the MC simulation

the temperatures of the given points. Then, the objective function in Eq. (5) is determined. The best parameters are considered to be the four heat generation rates corresponding to the minimum objective function value of k sampling times, that is, $F^* = \min(F_0, F_1, \cdots, F_{k-1})$, and the heat generation rates corresponding to F^* are denoted by x_1^*, x_2^*, x_3^*, and x_4^*.

Once the Monte Carlo simulation is finished, a judgment statement of the minimum objective function value is taken with a given accuracy ε. If the given accuracy is satisfied, then the calculation results of the heat generation rates are output and the computational procedure is ended. Otherwise, another judgment statement of distribution intervals for the heat generation rates is taken as the following

$$\min(\delta_1, \delta_2, \delta_3, \delta_4) < \delta_0 \tag{7}$$

where δ_0 is a given small constant.

If Eq. (7) is satisfied, the Monte Carlo simulation fails and the computational procedure is ended. Otherwise, the low and upper limits of the parameters are re-determined by Eq. (8) and the MC simulation is repeated.

$$\begin{aligned} \delta_l &= \frac{1}{2}\delta_l \\ x_{Ll} &= \begin{cases} x_l^* - \delta_l & \text{if } x_l^* - \delta_l > 0 \\ 0, & \text{otherwise} \end{cases}, l = 1, 2, 3, 4. \\ x_{Ul} &= x_l^* + \delta_l \end{aligned} \tag{8}$$

2.4 Temperature relationship between the measured point and the center of kinematic pairs

As aforementioned, it is difficult to measure the center temperatures of the kinematic pairs. But the center temperatures of the kinematical pairs are necessary to predict the thermal error

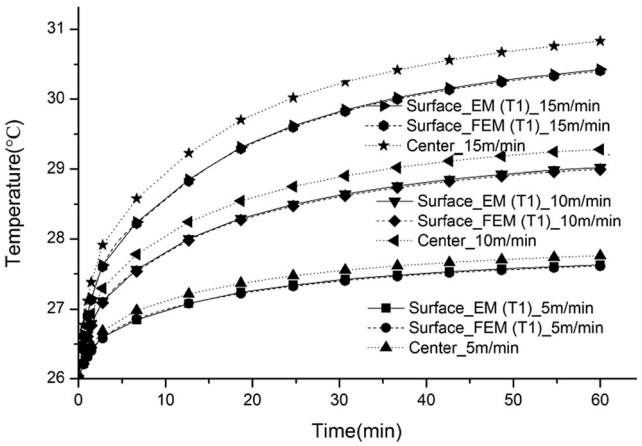

Fig. 4 Temperatures of the measured point T1 and the center of bearing 1

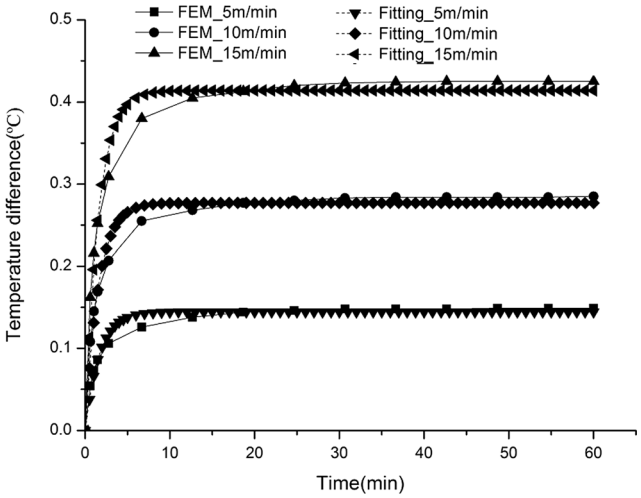

Fig. 5 Temperature differences between the measured surface point and the center of bearing 1

of the ball screw. This paper develops a model of the temperature relationship between the measured surface point and the center of the kinematical pairs based on the data of numeric simulation. Through many FE calculations with the heat generation rates obtained using the FEM/MC method, temperature variations of the measured point T1 and the center for bearing 1 with time were obtained, as shown in Fig. 4. As illustrated in Fig. 4, the temperatures of the FEM simulation on the surface point T1 of bearing 1 all match quite well with the experimental temperature curves for the feed velocities of 5, 10, 15 m/min. The temperature differences between the measured surface point and the center of bearing 1 are plotted in solid lines in Fig. 5 and show approximate index variations with time. Hence, based on the FE calculation data, the temperature difference between the measured surface point and the center of a kinematic pair used herein can be expressed as an exponential function of the feed velocity and time

$$\Delta T(t, v) = av\left(1 - e^{-t/bv}\right) \tag{9}$$

where v is the feed velocity of the x-worktable, t is the work time, and a and b are the constants obtained by curve fitting.

The exponential fitting curves for the temperature difference between the measured surface point and the center of bearing 1

Table 1 Parameters of exponential fitting curves and the maximum errors for the temperature differences between the measured surface point and the center of the kinematical pairs

Heat source	Coefficient		The maximum errors (°C)		
	a	b	5 m/min	10 m/min	15 m/min
Bearing 1	0.028	0.196	0.014	0.034	0.05
Bearing 2	0.027	0.195	0.015	0.032	0.045
Moving nut	0.025	0.201	0.016	0.036	0.048

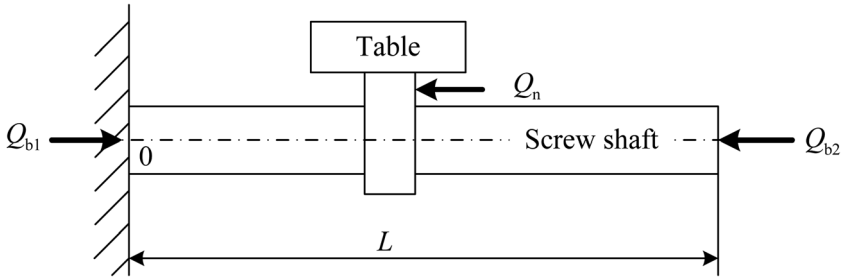

Fig. 6 Heat source of the screw shaft

are plotted in dash line in Fig. 5. Table 1 lists the parameters of exponential fitting curves and the maximum errors for the temperature differences between the measured surface points and the centers of the two bearings, and the moving nut at the feed velocities of 5, 10, and 15 m/min, respectively. The data in Table 1 and Fig. 5 demonstrate that Eq. (9) is general and suitable for the two bearings and the moving nut.

During the working process of x-worktable, the temperature of a given point on the surface of a kinematic pair can be continuously measured using a thermocouple in real time, the center temperature of the kinematic pair can be expressed as the following

$$T_c = T_m + \Delta T(t, v) \tag{10}$$

where T_c is the center temperature of the kinematic pair and T_m is the measured temperature of a given point on its surface.

3 Adaptive real-time model of the thermal error

3.1 Equation of heat conduction

As is well known, heat generation is the root of temperature rise and thermal deformation of the ball screw system. Heat affecting the thermal deformation of the screw shaft is mainly generated by the two bearings and the moving nut, as shown in Fig. 6. The thermal deformation of the screw shaft in the axial direction affects the machining accuracy of the machine tools. Hence, the thermal deformation of the screw shaft in the radial direction can be not taken into account. In this ball screw system, the down end of the ball screw was fastened, and the up end of it was free, as shown in Figs. 1 and 6. The equation of heat conduction of the screw shaft is expressed as

$$\begin{cases} \dfrac{\partial^2 T(x,t)}{\partial x^2} = \dfrac{\rho c}{\kappa}\dfrac{\partial T(x,t)}{\partial t} + \dfrac{4h}{\kappa d}\left(T(x,t) - T_f(t)\right) \\ T(x,0) = T_f(0) \\ T(0,t) = T_{b1}(t_j), \\ T(L,t) = T_{b2}(t_j) \\ T(x,t) = T_n(x_i, t_j) \\ T_f(x,t) = T_f(t_j) \end{cases} \quad x \in [0, 220] \tag{11}$$

where $T(x, t)$ is the temperature of the screw shaft, which is a function of time t and position x, κ is the thermal conductivity, ρ is the material density of the ball screw, and c is the specific heat capacity, h is the convection coefficient. $T_f(t)$ is the temperature of the ambient air.

The screw shaft is partitioned into mesh by a space step s and a time step τ, that is, $x_k = k \cdot s$, $k = 1, 2, \cdots, M$, $t_j = j \cdot \tau$, and $j = 1, 2, \cdots, N$. Denoting $T(x_k, t_j)$ as T_j^k, and inserting the finite difference equations of the first-order derivative and the second order derivative

$$\frac{\partial T_j^k}{\partial t} = \frac{T_j^{k+1} - T_j^k}{\tau} \tag{12}$$

$$\frac{\partial^2 T_j^k}{\partial x^2} = \frac{T_{j+1}^k - 2T_j^k + T_{j-1}^k}{s^2} \tag{13}$$

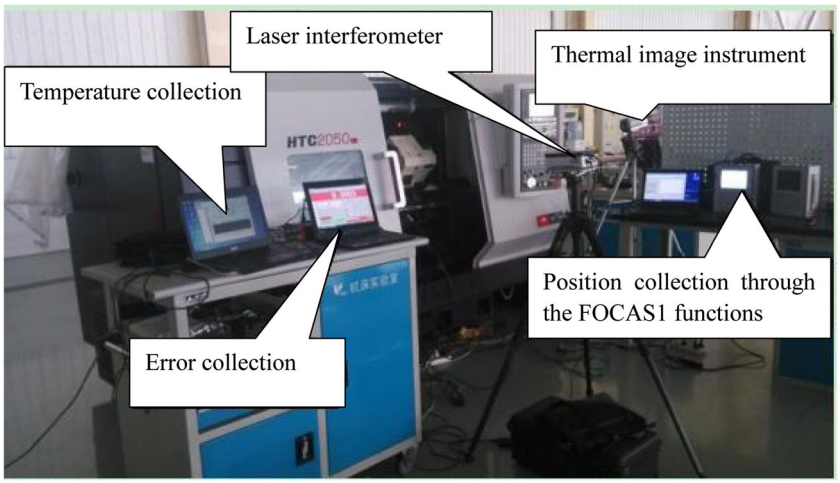

Fig. 7 Photograph of the experimental setup

Table 2 Specification for the *X*-axis feed drive system of the CNC lathe

Parameters	Value
Mass of working table	50 kg
Model of ball screw	3210
Diameter	32 mm
Lead of screw	10 mm
Stroke	220 mm
Nut length	80 mm
Nut type	Single nut
Bearing type	Contact ball bearing
Inner diameter	30 mm
Outer diameter	62 mm
Mean diameter	46 mm
Width	16 mm
Lubrication	Grease

into Eq. (11) and rearranging it, one can get:

$$T_{j+1}^{k+1} = \frac{\tau}{As^2} T_{j+1}^{k} + \left(\frac{As^2 - Bs^2 - 2\tau}{As^2}\right) T_j^k + \frac{\tau}{As^2} T_{j-1}^{k} - \frac{Bs^2}{As^2} T_f(j) \quad (14)$$

where $A = \rho c/\kappa$ and $B = 4h/(\kappa d)$.

If $(As^2 - Bs^2 + 2\tau)/(As^2) \geq 0$, i.e., $(\tau/s^2) \leq (A - B)/2$, then Eq. (14) is stable.

According to Eq. (10), the temperature for the center of the two bearings can be expressed as

$$T_{cbl} = T_{mbl} + \Delta T_{bl}(t, v), \quad l = 1, 2. \quad (15)$$

and the temperature of the moving nut center can be expressed as

$$T_{cn} = T_{mn} + \Delta T_{n}(t, v) \quad (16)$$

3.2 Thermal error of the screw shaft

During the machining process, the screw shaft will elongate due to a rise in internal temperature caused by frictional heat. The thermal elongation value can be expressed as follows:

$$\Delta L = L \cdot \alpha \cdot \Delta T \quad (17)$$

where L is the length of the screw shaft.

Hence, the thermal elongation value of the screw shaft at the position of x can be expressed as follows:

$$\Delta L(x) = \alpha \int_0^x \Delta T(x, t) \mathrm{d}x \quad (18)$$

where $\Delta L(x)$ indicates the thermal elongation value at time of t, $\Delta T(x, t)$ denotes the temperature variation of the screw shaft, and α is the coefficient of linear thermal expansion.

4 Experimental setup and procedure

To study the thermal characteristics of ball screw systems, an experiment was carried out on the *X*-axis ball screw of a slant bed lathe with Fanuc Series 0i Mate-TD, as shown in Fig. 7. The parameters of the ball screw are listed in Table 2.

Temperatures were measured in two ways: the surface points of T1, T8, and T9 were measured using three T-type thermocouples, the points of T2–T7 and T10–T15 were measured using an infrared thermographic camera with high precision (0.1°C), as shown in Figs. 2 and 7. The three thermocouples were attached to the surfaces of the bearing seats 1 and 2 and the nut flank with their magnetic bases, respectively, and their data were collected by using a portable computer with sampling cycle of 0.5 s. A PC 104 computer with the Visual C++ FOCAS1 application was used to record the position of the moving nut during the working process of the worktable.

According to the measuring criterion of ISO230-2 [26] and ISO230-3 [27], a laser interferometer was used to measure the *X*-axis positioning error. The machine reference origin was set to be the starting point for this measurement, and the positioning error was measured every 44 mm in the whole stroke range of 220 mm, i.e., the worktable located at the points P1–P6 shown in Fig. 8. Firstly, the initial geometric error was measured at normal temperature when the machine tool was

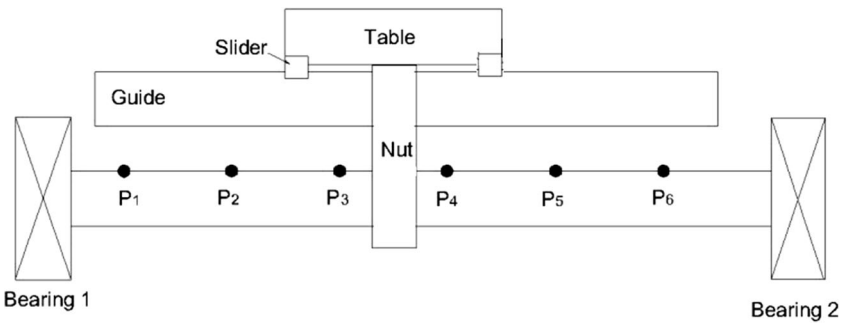

Fig. 8 Distribution of measured points for the screw thermal error

initially switched on. Then, the machine tool was warmed up by moving the *X*-axis worktable along its stroke range with a given feed velocity. Meanwhile, the temperatures of points T1, T8, and T9 were recorded with a sampling interval of 0.5 s. In addition, picture of the screw shaft and the two guides was taken by the thermographic camera at an interval of 10 min. And the positioning error was measured synchronously after the machine tool had been warmed up for 10, 20, 30, 40, and 50 min, respectively. In this study, three idling experiments were conducted at the feed velocities of 5, 10, and 15 m/min, respectively. Each experiment was started under the condition of the environmental temperature and the worktable moved forward and backward over the whole stroke range.

5 Results and discussions

During the working process of the worktable, the position sampling cycle of the PC 104 computer was 48 ms, which depended on the application program speed [28, 29], so the time step in Section 3 was assumed to be $\tau = 0.048$ s. The other parameters of the ARTM were: $\kappa = 43.3$ W/m°C, $\rho = 7800$ kg/m^3, $s = 0.022$ m, $d = 0.032$ m, and $M = 10$.

Figure 9 shows the results of the ARTM, the FEM, and the experiment for the *X* screw shaft temperatures during the working process of the worktable at the feed velocity of 10 m/min. It can be seen from Fig. 9 that both the calculation curves of the ARTM and the FEM could match quite well with the measured temperatures.

Figure 10 shows comparison of the positioning errors calculated by the ARTM and the FEM with the measured results. As illustrated in Fig. 10, the calculated positioning errors of both the two models could also match quite well with the actual measured error, and their accuracies all turn out to be satisfactory. But the calculation time of the FEM was about 45 min, and that of the ARTM was only about 120 ms, that is, the calculation time of the FEM was far greater than that of the ARTM. So, the ARTM proposed in this paper is suitable for rapidly predicting the positioning error with high accuracy.

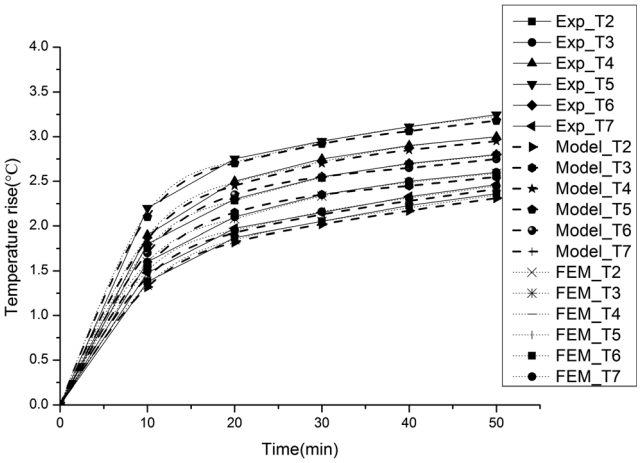

Fig. 9 Comparison of temperature rise for FEM and ARTM calculations, and experimental results under the feed velocity of 10 m/min

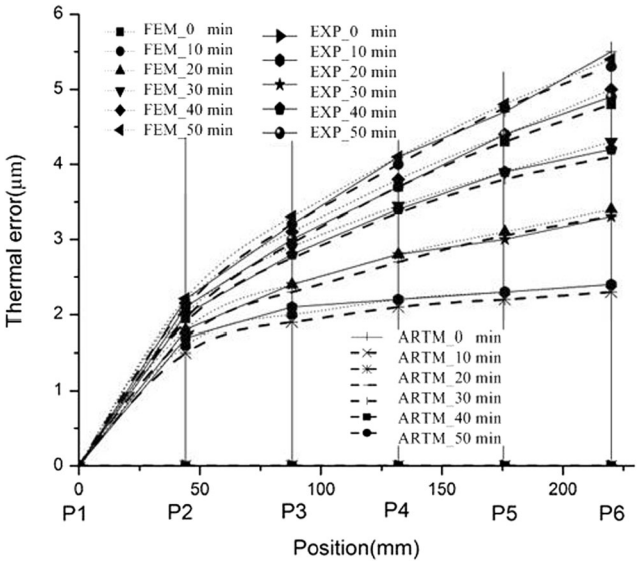

Fig. 10 Comparison of thermal error for FEM and ARTM calculations, and experimental results under the feed velocity of 10 m/min

6 Conclusions

From the numeric analysis and experimental results in the above sections, the following remarks can be stressed.

The FEM integrated with the Monte Carlo method proposed in this paper can be used to predict the heat flow rates, the temperature distribution, and the thermal errors of ball screw feed drive systems. The temperature difference between the measured surface point and the center of the kinematic pair can be expressed as an exponential function of the feed velocity v and time t, of which the parameters can be determined by fitting the data of the FEM integrated with the Monte Carlo.

The proposed ARTM can be used to predict the thermal error of ball screw feed drive system. By monitoring the surface temperatures of the two bearing seats and the moving nut flank, the ball screw temperature field is derived using the numerical forecasting algorithm, and the corresponding positioning error can also be predicted with high accuracy.

Acknowledgements This work was supported by the National Natural Science Foundation of China under grant 51375081. Simultaneously, it was supported by the important national science & technology specific projects 'High-end CNC machine tools and basic manufacturing' of China under grant 2013ZX0401-011.

References

1. Shi H, Ma C, Yang J, Zhao L, Mei XS, Gong GF (2015) Investigation into effect of thermal expansion on thermally induced error of ball screw feed drive system of precision machine tools. Int J Mach Tools Manuf 97:60–17
2. Bryan J (1990) International status of thermal error research. CRIP Ann Manuf Techn 39(2):645–656
3. Ramesh R, Mannan MA, Poo AN (2003) Thermal error measurement and modeling in machine tools. Part I: influence of varying operation condition. Int J Mach Tools Manuf 43:391–404
4. Mayr J, Jedrzejewsk UE, Donmez MA, Knapp W, Härttig F, Wendt K, Moriwaki T, Shore P, Schmitt R, Brecher C, Würz T, Wegener K (2012) Thermal issues in machine tools. CIRP Ann-Manuf Techn 61:771–793
5. Du ZC, Yang GJ, Yao ZQ, Xue BY (2002) Modeling approach of regression orthogonal experiment design for the thermal error compensation of a CNC turning center. J Mater Process Tech 129:619–623
6. Schwenke H, Knapp W, Haitjeme H, Weckenmann A, Schmitte R, Delbressine F (2008) Geometric error measurement and compensation of machines—an update. CRIP Ann Manuf Techn 57(2): 660–675
7. Xu ZZ, Liu XJ, Kim HK, Shin JH, Lyu SK (2011) Thermal error forecast and performance evaluation for an air-cooling ball screw system. Int J Mach Tools Manuf 51:605–611
8. Wu H, Zhang HT, Guo QJ, Wang XH, Yang JG (2008) Thermal error optimization modeling and real-time compensation on a CNC turning center. J Mater Process Tech 207:172–179
9. Xu ZZ, Liu HJ (2014) Study on thermal behavior analysis of nut/shaft air cooling ball screw for high-precision feed drive. Int J Precis Eng Man 15(1):123–128
10. Tanabe I, Takada K (1994) Thermal deformation of machine tool structures using resin concrete. Jpn Soc Mech Engrs C 37(2):384–389
11. Moriwaki T (1988) Thermal deformation and its on-line compensation of hydrostatically supported precision spindle. CIRP Ann-Manuf Techn 37(1):393–396
12. Ramesh Babu S, Prabhu Raja V, Thyla PR, Thirumalaimuthukumaran M (2014) Prediction of transient thermo-mechanical behavior of the headstock assembly of a CNC lathe. Int J Adv Manuf Technol 74:17–24
13. Yeh SS, Su HC (2011) Development of friction identification methods for feed drives of CNC machine tools. Int J Adv Manuf Technol 52:263–278
14. Tan B, Mao XY, Liu HQ, Li B, He SP, Peng FY, Yin Y (2014) A thermal error model for large machine tools that considers environmental thermal hysteresis effects. Int J Mach Tools Manuf 82-83:11–20
15. Lee JH, Lee JH, Yang SH (2001) Thermal error modeling of a horizontal machining center using fuzzy logic strategy. J Manuf Process 3(2):120–127
16. Venugopal R, Barash M (1986) Thermal effects on the accuracy of numerically controlled machine tools. CRIP Ann Manuf Techn 35(1):255–258
17. Week M, Zangs L (1975) Computing the thermal behavior of machine tools using the finite element method-possibilities and limitations. Proceedings of the 16th MTDR Conference 16:185–194
18. Wu CH, Kung YT (2003) Thermal analysis for the feed drive system of a CNC machine center. Int J Mach Tools Manuf 43:1521–1528
19. Kim SK, Cho DW (1997) Real-time estimation of temperature distribution in a ball-screw system. Int Mach Tools Manuf 37(4):451–464
20. Heisel U, Koscsak G, Stehle T (2006) Thermography-based investigation into thermally induced positioning errors of feed drives by example of a ball screw. CRIP Ann Manuf Technol 55(1):423–426
21. Min X, Jiang S (2011) A thermal model of a ball screw feed drive system for a machine tool. Proc IMechE Part C: J Mech Eng Sci 225:187–193
22. Li ZH, Fan KG, Yang JG, Zhan Y (2014) Time-varying positioning error modeling and compensation for ball screw systems based on simulation and experimental analysis. Int J Adv Manuf Technol 73: 773–782
23. Jedrzejewski J, Modrzycki W (1992) A new approach to modelling thermal behaviour of a machine tool under service conditions. CRIP Ann Manuf Techn 41(1):455–458
24. Yun WS, Kim SK, Cho DW (1999) Thermal error analysis for a CNC lathe feed drive system. Int J Mach Tools Manuf 39:1087–1101
25. Brooks SP (1998) Markov chain Monte Carlo method and its application. Underst Stat 47:69–100
26. ISO230-2:2006. Test code for machine tools—part 2: determination of accuracy and repeatability of positioning numerically controlled axes. International Standards Organization
27. ISO230-3:2007. Test code for machine tools—part 3: determination of thermal effects. International Standards Organization
28. Chen Y, Zhao CY, Zhang YM, Wen BC (2017) On the friction characteristics of CNC machine tool's feed drive system. Journal of Northeastern University (Natural Science) 38(7):993–997 **(in Chinese)**
29. FANUC, FOCAS1: FANUC Open CNC API Specifications version 1-FOCAS1/Ethernet CNC/PMC Data window library, http://www.graco.unb.br/alvares/romi/Focas1/Disk2/Doc/FWLIB32.htm, 2003